JOURNAL OF PROPULSION AND POWER
Vol. 9, No. 6, Nov.–Dec. 1993

Hydraulic and Mechanical Performance of LE-7 LOX Pump Inducer

Kenjiro Kamijo,* Makoto Yoshida,† and Yoshinobu Tsujimoto‡
National Space Laboratory, Kakuda, Miyagi 981-15, Japan

A liquid oxygen turbopump has been developed for the main engine (LE-7) of the H-II rocket. The LE-7 LOX pump requires an inducer with quite high suction performance and high head, because a low-speed and low-pressure pump is not used ahead of the main pump in the LE-7 engine. The inducer was designed using the customary method, and its hydraulic and mechanical performances were investigated in tests of LE-7 LOX turbopumps. The original combination of an inducer and an inducer housing satisfied the required hydraulic performance criteria. However, this combination was found to result in supersynchronous shaft vibrations due to rotating cavitation which occurred in the inducer. This problem was almost completely solved by a simple modification of the inducer upstream housing. Furthermore, the rotating cavitation of the present inducer was investigated using a new theory of such cavitation.

I. Introduction

A LIQUID oxygen turbopump has been developed for the main engine (LE-7) of the H-II rocket, the next generation of Japanese launch vehicle. This turbopump requires a high-flow, high-pressure liquid oxygen pump. Because a low-speed, low-pressure pump is not used ahead of the main pump in the LE-7 engine, it is very important to operate the main pump at higher speed to obtain a smaller-size, lighter-weight turbopump. The operational speed of the present turbopump was restricted by the suction performance of the main pump inducer. In this article, we report both the design and test results of the inducer.

The main pump of the LE-7 LOX turbopump has a single-stage centrifugal impeller with an inducer.[1] The inducer is characterized by a low flow coefficient, a small inlet angle, a sharp leading edge, etc., to achieve higher suction performance. The inducer was designed using the customary method.[2,3]

The inducer showed almost no decrease of head coefficient, even at cavitation number $\sigma[=2(p_i - p_v)/\rho W_i^2] = 0.014$ ($S \cong 2.40$), where p_i, p_v, ρ, and W_i are inducer inlet pressure, vapor pressure of pump fluid, density of pump fluid, and inducer inlet relative velocity. It means that it could hydrodynamically satisfy the design suction performance criteria. However, the head coefficient curve was not stable at cavitation numbers in the range of 0.02–0.05. In the same range of cavitation numbers, supersynchronous shaft vibrations or jumps in amplitude of the synchronous shaft vibrations were observed. The ratios of these vibration frequencies to the inducer rotational frequencies were 1.0–1.2. From a comparison with results of previous studies[4–6] on rotating cavitation, it was concluded that such shaft vibration was caused by rotating cavitation in the inducer.

Effort was made to suppress the rotating cavitation. Increasing tip clearance was found to be fairly effective in preventing such cavitation, but could not extinguish it. A suction ring, which is usually used to control the backflow at the inducer inlet, was very effective in suppressing such cavitation. However, since a large number of tests were required to confirm the durability of this ring, it was not applied to the flight model turbopump. A simple modification of the inducer upstream housing almost completely extinguished not only such shaft vibration, but also the unstable region of the head coefficient curve. Recently, a new theory of rotating cavitation has been proposed by Tsujimoto et al.[7] Using this theory, the rotating cavitation of the present inducer was investigated.

II. LE-7 LOX Main Pump and Its Inducer

Figure 1 presents the mechanical configuration of the LE-7 LOX turbopump. It consists of a main pump and a preburner pump which are driven by a single-stage gas turbine. Table 1 presents design parameters of the LE-7 main pump. The main pump has a single-stage impeller with an inducer. The large flow rate and high suction specific speed require an increased inlet diameter of the inducer. Therefore, the inducer and the main pump impeller were arranged as shown in Fig. 1. The guide vanes between the inducer and the main impeller were utilized to support the housing for self-lubricated ball bearings.

The major design parameters of the inducer are presented in Table 2. This inducer with three helical blades is characterized by a low flow coefficient, which requires a small inlet angle. The small inlet angle also requires a sharper leading edge to reduce cavitation blockage for achieving higher suction performance. A computer program[3] was used to obtain the pressure distribution of blade surfaces, such data being necessary for structural analysis of the inducer. The inducer profile consists of a flat plate blade at the entrance and a circular arc blade in the remainder. The geometrical dimensions of the leading edge are presented in Table 3. R, Z_s, β, α_w, and T_0 are radius, axial distance of sweepback, blade angle, blade wedge angle at the leading edge, and blade thickness, respectively.

A comparatively large sweepback was necessary in order to decrease high stresses at the hub near the leading edge. Figure 2 shows the calculated stresses of the inducer blades. The maximum stress was more than 1000 MPa, even though the blade near the hub was fairly thick. This led to the decision to use an inducer machined from heat resisting alloy (Inconell 718) which shows higher strength at cryogenic temperatures.

Presented as Paper 92-3133 at the AIAA/SAE/ASME/ASEE 28th Joint Propulsion Conference and Exhibit, Nashville, TN, July 6–8, 1992; received Aug. 4, 1992; revision received May 26, 1993; accepted for publication June 3, 1993.

*Deputy Director and Head of Rocket Fluid Systems Section, Kakuda Research Center. Member AIAA.

†Research Engineer, Kakuda Research Center. Member AIAA.

‡Visiting Researcher, Kakuda Research Center; on leave from Osaka University, Engineering Science Professor, Toyonaka, Osaka 560, Japan. Member AIAA.

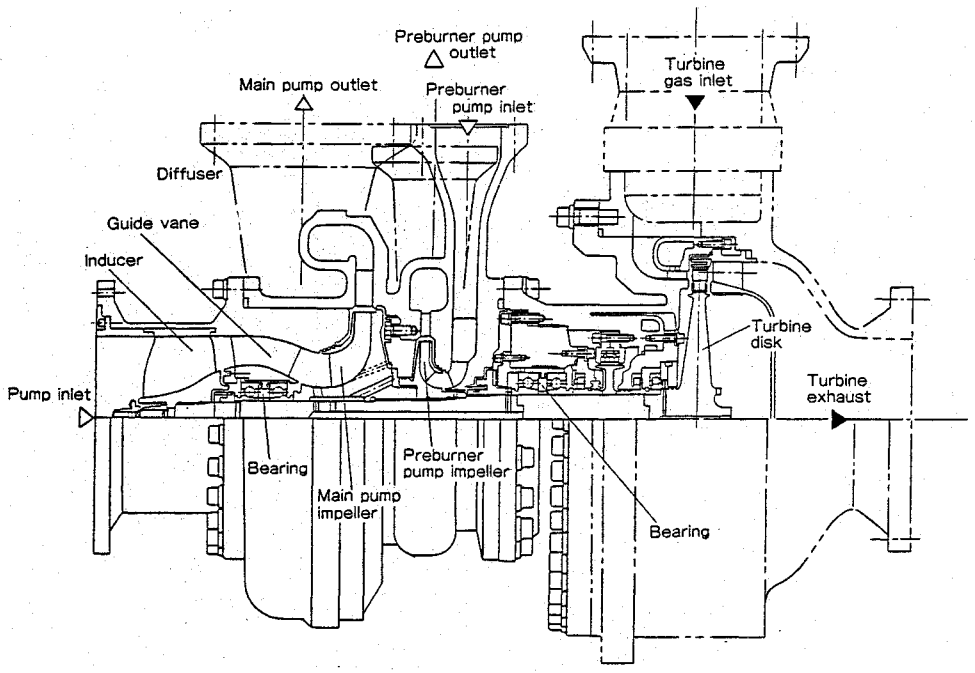

Fig. 1 LE-7 LOX turbopump.

Table 1 Major design parameters of LE-7 main pump

Rotational speed, rpm	20,000
Main pump	
Required NPSH, m	30
Mass flow, kg/s	229.1
Pressure rise, MPa	20.9
Efficiency, %	75

Table 2 Design parameters of LE-7 main pump inducer

Rotational speed N, rpm	20,000
Required NPSH, m	30.0
Suction specific speed S, m, m^3/s, s^{-1}	2.10
Cavitation number σ	0.017
Number of blades	3
Inlet flow coefficient,[a] ϕ_1	0.083
Outlet flow coefficient[a] ϕ_2	0.104
Inducer head coefficient[a] Ψ	0.097
Tip diameter D_t, mm	149.8
Inlet tip blade angle β_{t1}, deg	7.50
Outlet tip blade angle β_{t2}, deg	9.50

[a]Values for 1.07 times the quantity of nominal flow.

Table 3 Geometrical dimensions of inducer leading edge

Radius R, mm	Axial distance of sweepback Z_s, mm	Blade angle β_1, deg	Blade wedge angle α_w, deg	Blade thickness T_0, mm
18.73	0.0	27.68	10.50	6.13
20.00	0.03	26.25	10.22	5.98
30.00	1.61	18.20	7.96	4.75
40.00	3.04	13.84	5.70	3.52
50.00	4.93	11.16	4.86	3.08
60.00	6.92	9.33	4.01	2.65
70.00	10.42	8.02	3.16	2.21
74.90	14.22	7.50	2.75	2.00

Structural analysis clearly showed that the blades were slightly deformed, due to both hydraulic and centrifugal forces, but this deformation was neglected in the design.

Five kinds of the inducer housings with dimensions shown in Fig. 3 and Table 4 were tested in order to find a method to suppress the rotating cavitation.

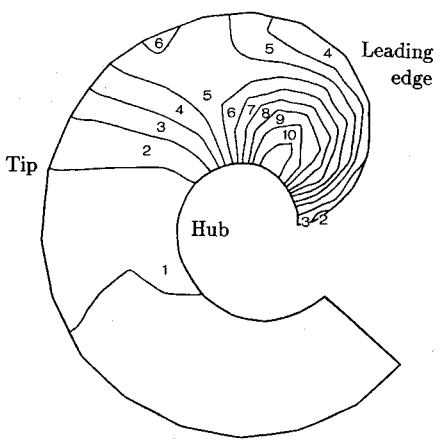

Figures indicate stress ($\times 10^2$ MPa)

Fig. 2 Calculated stress of inducer blade.

III. Test Facility and Procedures

Data on the inducer were obtained during the operation of the LE-7 LOX turbopump. Tests of the turbopump were performed using the high-pressure LOX turbopump test facility which was constructed in 1986. A schematic diagram of the facility is shown in Fig. 4. The duration of the LE-7 LOX turbopump test using this facility is about 20 s. High pressure gaseous hydrogen (GH_2) at room temperature and LOX pressurized by gaseous helium are supplied to a gas generator which produces the turbine working fluid.

The flow rate through the inducer was obtained as a sum of flow rates of the main pump and split pump, which were measured by turbine-type flow meters. Cryogenic temperatures of the pump fluid were measured by C-C thermocouples. The thermocouples were calibrated by an apparatus which was designed utilizing the relation between saturated vapor pressures and temperatures. Pressure measurements were carried out with strain-gauge-type sensors. Rotational speed was measured with a combination of a toothed wheel set in the LOX turbopump shaft and a magnetic pulse pick-up. Information on cryogenic fluid properties, necessary for evaluating inducer hydraulic performance, was obtained from handbooks.[8,9] The displacement of the main pump impeller

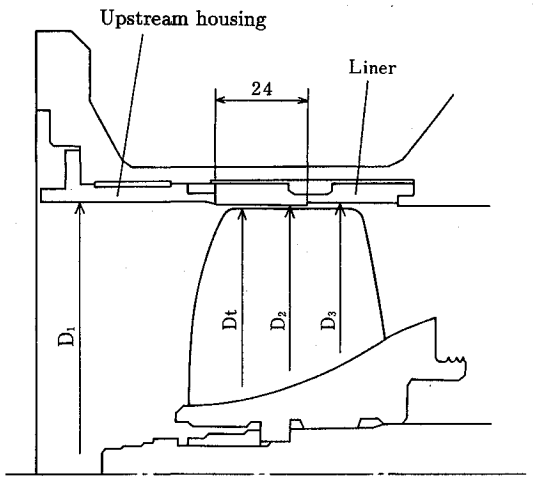

Fig. 3 Details of inducer housing.

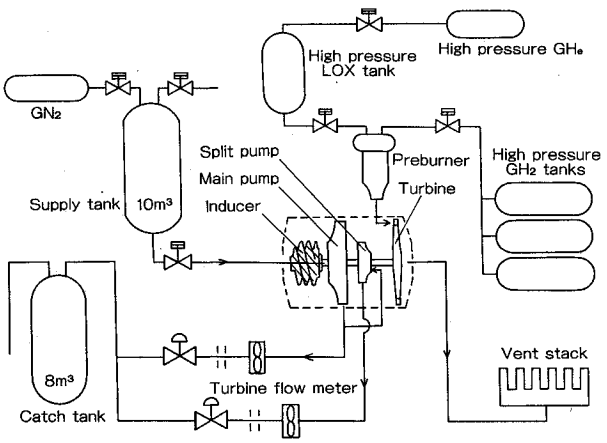

Fig. 4 LE-7 LOX turbopump test facility.

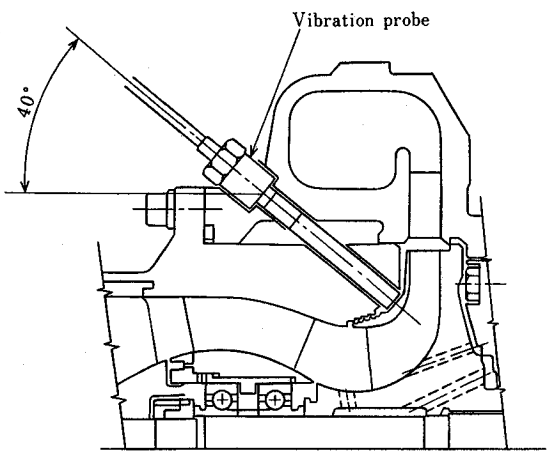

Fig. 5 Displacement measurement probe.

Table 4 Dimensions of inducer housing

	Inside diameter of upstream housing D_1, mm	Inside diameter of first half of liner D_2, mm	Inside diameter of latter half of liner D_3, mm
Housing A	150.8	150.8	151.4
Housing B	151.3	151.3	151.3
Housing C	153.0	151.3	151.3
Housing D	149.8	150.8	150.8
Housing E	149.8	151.8	151.8

was measured by an eddy-current-type sensor as shown in Fig. 5.

IV. Relationship Between Suction Performance and Shaft Vibrations

The relationship between cavitation number, σ and inducer head coefficient, $\psi(=gH/U_t^2)$, is presented in Fig. 6, where g, H, and U_t are acceleration due to gravity, inducer total head, and peripheral velocity of inducer, respectively. Crosses (+) indicate values when the original inducer housing (inducer housing A) was used, and circles (○) represent values when the modified inducer housing (inducer housing C) was used. Each head coefficient curve was obtained at a constant rotational speed and with a constant flow rate by reducing the inducer inlet pressure. The sum of static head and dynamic head at the outlet of the inducer guide vanes was used as a substitute for the inducer outlet total head which was necessary to obtain the inducer head coefficient. There was almost no degradation of head coefficient, even at the cavitation number of $\sigma \cong 0.014$ ($S = 2.40$), which completely satisfied the designed suction performance criteria. However, the head coefficient curve presented by + symbols was not flat at the cavitation numbers of $\sigma = 0.02$–0.05. There was remarkable head degradation near the cavitation number of $\sigma = 0.027$.

Figure 7 shows a spectrum analysis of the displacement of the main pump impeller obtained by the same test as that which yielded the data of + symbols in Fig. 6. A supersynchronous vibration and amplitude jump of synchronous vibration were evident. They occurred in the same range of cavitation numbers, $\sigma = 0.02$–0.05, where the previously mentioned inducer head degradation occurred. In particular, both the remarkable head degradation and the amplitude jump of synchronous vibration occurred simultaneously, that is at

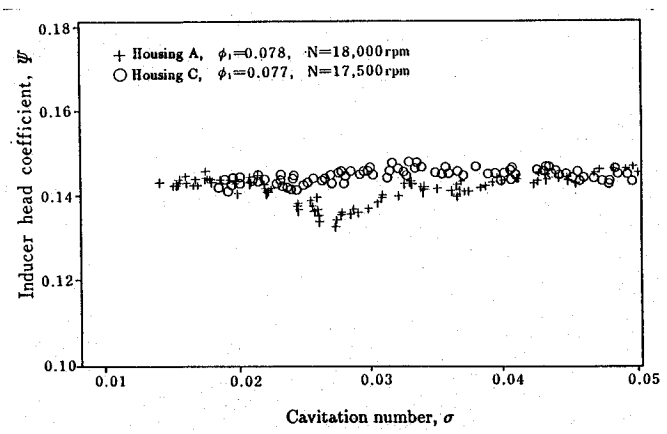

Fig. 6 Suction performance of LE-7 main pump inducer.

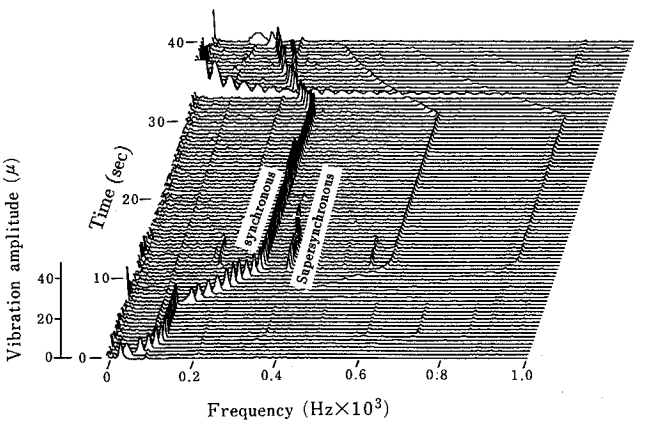

Fig. 7 Spectrum analysis of main pump impeller displacements (inducer housing A).

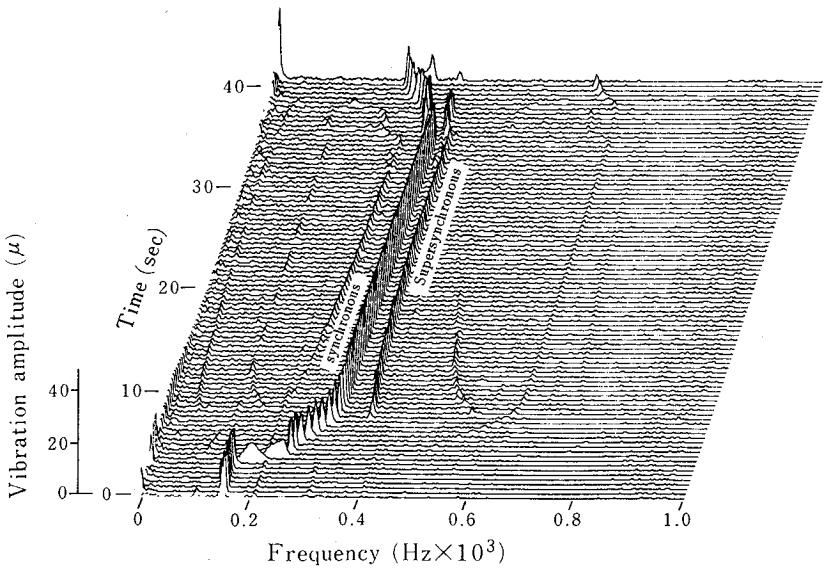

Fig. 8 Spectrum analysis of main pump impeller displacements (inducer housing A).

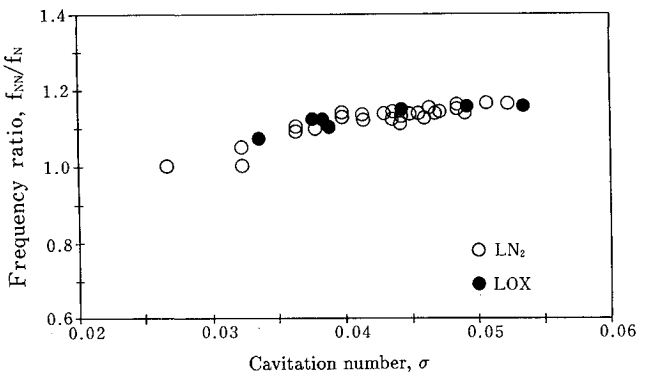

Fig. 9 Frequency of supersynchronous vibrations.

the same cavitation number of $\sigma = 0.027$. Figure 8 presents other supersynchronous vibration data for a relatively high range of cavitation numbers, $\sigma = 0.045$–0.055. The same kind of vibrations were observed in almost all the LOX turbopump tests in which the original inducer housing was used. The ratio of this vibration frequency f_{NN} to the inducer rotational frequency f_N was 1.0–1.2, and tended to decrease along with the decrease of cavitation number as shown in Fig. 9.

From a comparison of the facts mentioned previously, a former study on rotating cavitation in an inducer reported by Kamijo et al.[4,5] and the experimental investigation of hydrodynamically induced shaft forces with an inducer reported by Rosenman[6] (introduced in the Appendix), it was concluded that the supersynchronous vibrations and the amplitude jump of the synchronous vibrations were caused by the rotating cavitation in the inducer.

V. Suppression of Rotating Cavitation

It was conjectured that rotating cavitation might be closely related to the tip vortex cavitation of an inducer, judging from the visual observations outlined in the Appendix. Some efforts were made to influence the tip vortex cavitation in the present inducer. Firstly, the influence of tip clearance on the supersynchronous shaft vibration was investigated by using inducer housings D and E shown in Table 4. The tip clearances for housings D and E are 0.5 and 1.0 mm, respectively. Increasing the tip clearance was fairly effective in decreasing the amplitude of the supersynchronous shaft vibration as shown in Fig. 10, but it could not completely distinguish the vibration. Acosta[10] previously reported that increasing the tip vortex cavitation helped prevent oscillating cavitation to some extent. Secondly, the suction ring shown in Fig. 11, which is usually used to control the back flow at the inducer inlet,[11] was also very effective in suppressing the supersynchronous vibration. There were some instances in which the vibration was completely extinguished. In spite of the remarkable effectiveness of the suction ring in suppressing the rotating cavitation, it was not applied to the flight model turbopump because it required a large number of tests to confirm its durability. Lastly, the influence of the inducer upstream housing diameter on supersynchronous vibrations was investigated. We obtained a very interesting relation of the inducer housing dimensions represented by the following equation, which almost completely extinguished the supersynchronous vibration, i.e., the rotating cavitation:

$$D_1 \geq D_2 + 2C_2 = D_2 + (D_2 - D_t) \qquad (1)$$

Figure 12 presents a spectrum analysis of the displacement of the main pump impeller in the test using inducer housing C ($D_1 \cong D_2 + 2C_2$). This device was applied to the flight model turbopump since there were no durability problems. It was confirmed that the device was very effective in suppressing the supersynchronous shaft vibration in the LE-7 engine test as shown in Fig. 13. The frequency of the supersynchronous shaft vibration scarcely changed because the inducer inlet pressure was kept almost constant during the test. It might be concluded that the mechanism of the modification of the inducer upstream housing for preventing the rotating cavitation is exactly the same as that of the suction ring. The head coefficient curve shown by circles (○) in Fig. 6 did not have the dent part which appeared in the head coefficient curve shown by crosses (+), which indicated that it was also caused by the rotating cavitation in the inducer.

Recently, Tsujimoto et al.[7] proposed a theory of rotating cavitation. In order to compare the rotating cavitation in the present inducer with theoretical results, calculations were done for the cavitation number of $\sigma = 0.04$ using Eq. (12) of Ref. 7. Parameters of the present inducer required for the calculations are presented in Table 3 of Ref. 7. Figure 14 is a contour map of rotating cavitation with a propagation velocity faster than the shaft rotational speed, which is defined as k_2^* rotating cavitation in Ref. 7. $|K|$ and $|M|$ are the absolute values of the cavitation compliance and mass flow gain factor, respectively. In this figure, k_R^* and k_I^* are the propagation velocity ratio (rotational velocity of rotating cavitation/inducer rotational speed) and the damping rate of the disturbance, respectively. In this calculation phase delays of cavity volume changes with frequency were considered utilizing Fig.

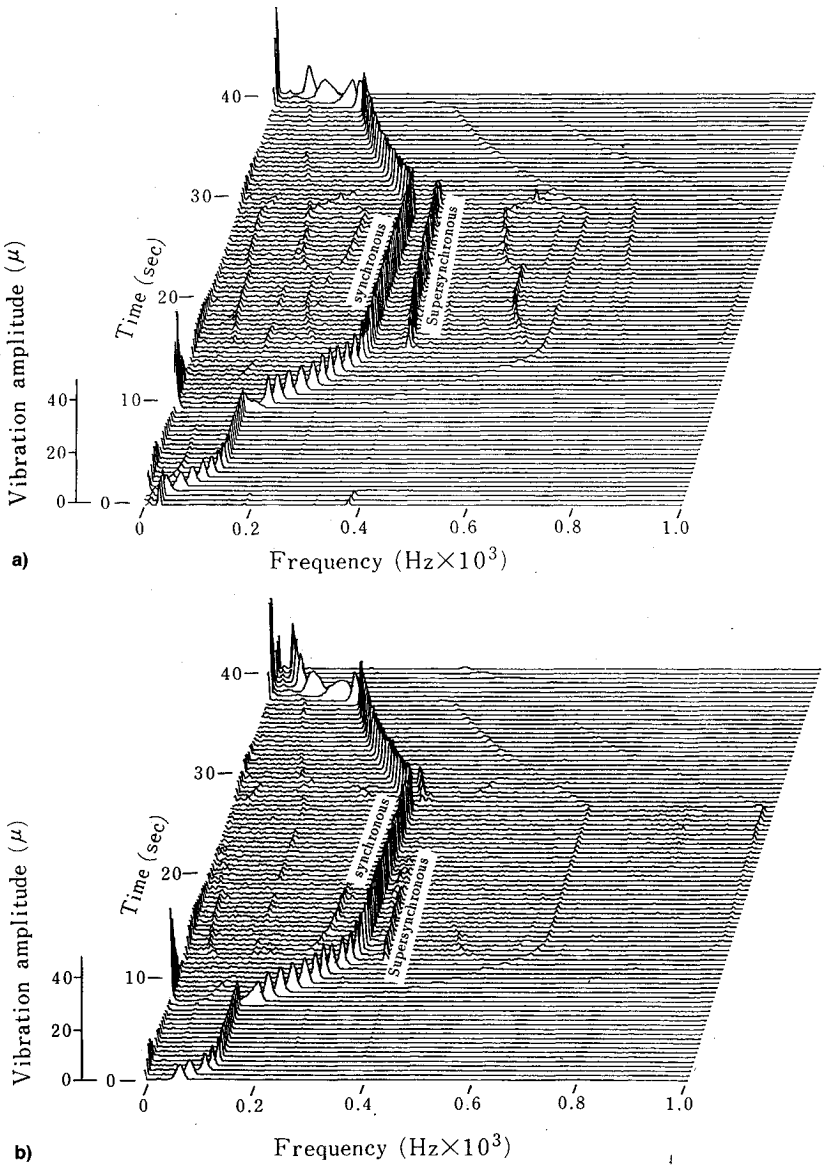

Fig. 10 Influence of tip clearance on supersynchronous vibrations: a) housing D (tip clearance = 0.5 mm) and b) housing E (tip clearance = 1.0 mm).

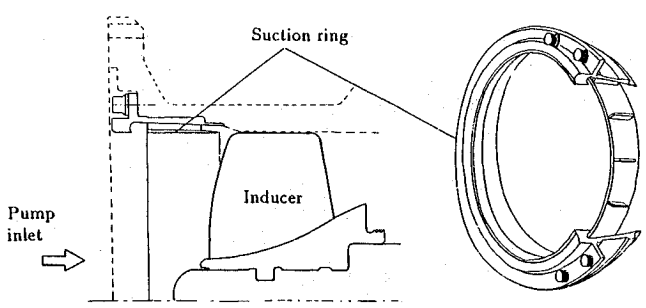

Fig. 11 Suction ring.

14 of Ref. 12. The ranges of M and K estimated from Eqs. (10) and (11) of Ref. 12 for three values of the cavitation number are also shown in Fig. 14. The estimated ranges shift to the location with smaller propagation velocity, which, however, is faster than the inducer rotational speed in the amplified range with reduction of the cavitation number. The estimated propagation velocity of $k_R^* = 1.2-1.4$ for $\sigma = 0.04$ is fairly close to the values of f_{NN}/f_N in Fig. 10.

Later, another experiment was performed to determine both the cavitation compliance and mass flow gain factor for the original and modified inducer upstream housings of the LE-7 LOX pump.[13] The cavitation compliance and the mass flow gain factor for the modified housing (housing C) were respectively much larger and a little smaller than those for the original housing (housing A). According to the present theory, the rotating cavitation of the present inducer seems to be suppressed by the increase of cavitation compliance and the decrease of mass flow gain factor.

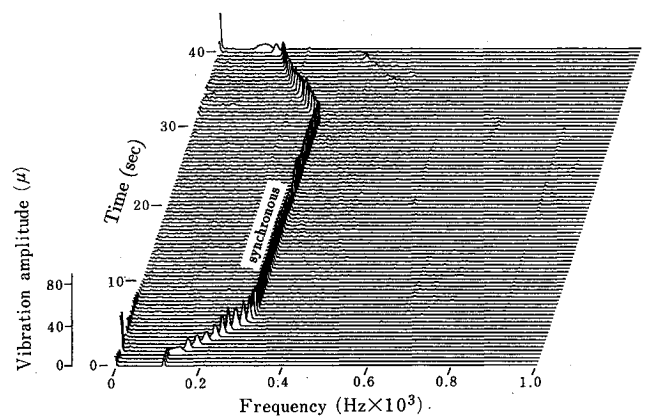

Fig. 12 Spectrum analysis of main pump impeller displacement (inducer housing C).

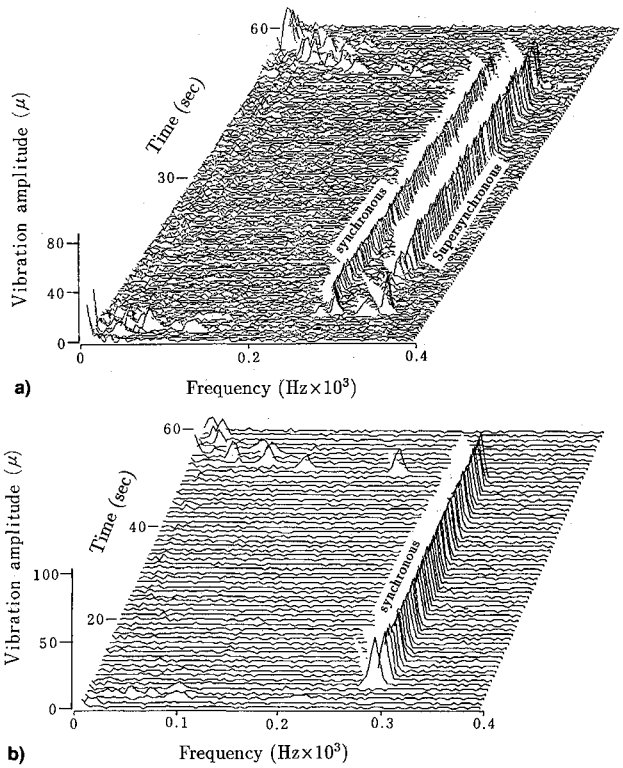

Fig. 13 Main pump impeller displacement in LE-7 engine test: a) original inducer housing and b) modified inducer housing.

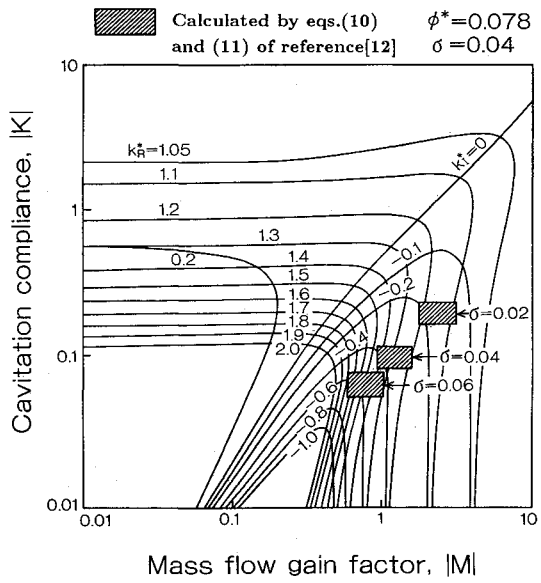

Fig. 14 Contour map of rotating cavitation with LE-7 main pump inducer.

VI. Concluding Remarks

The LE-7 LOX main pump requires an inducer with quite high suction performance and high head. The inducer was designed using the customary method, and its hydraulic and mechanical performances were investigated in the tests of the LE-7 LOX turbopumps. Major results of this work are as follows:

1) The inducer satisfied the required suction performance criteria, namely almost no decrease of head coefficient even at the cavitation number of $\sigma = 0.014$.

2) The original inducer housing resulted in an unstable head coefficient curve at the cavitation number of $\sigma = 0.02$–0.05, where supersynchronous shaft vibration or an amplitude jump of the synchronous shaft vibration was also observed.

3) Comparisons with previous reports made it clear that item 2 was due to the rotating cavitation of the inducer.

4) A simple modification of the inducer upstream housing almost completely extinguished the problem mentioned in item 2, namely the rotating cavitation of the present inducer.

5) A new theory of rotating cavitation proposed by Tsujimoto et al.[7] fairly well explained the main characteristics of the rotating cavitation of the present inducer.

Appendix: Features of Rotating Cavitation

Some features of rotating cavitation were fairly well clarified by an experiment mainly based on visual observation of a cavitating inducer whose dimensions are described in Table A1. Figure A1 presents the head coefficient curve of the inducer. Rotating cavitation occurred within specific regions of the cavitation number and tended to occur as the flow coefficient decreased. Figure A2 shows high-speed motion pictures of a typical example of rotating cavitation. Pictures were picked up at every one-third turn of the blades and arranged so as to show the cavity size on each blade at every turn. Therefore, the sequence of blades numbers is 1, 2, 3. Three series of pictures present one cycle cavity oscillations for each blade. Figure A3 presents the variation of the approximate cavity length with time. The cavity length was measured from high-speed motion film. Both the tip and blade surface cavities on one blade oscillated with almost the same frequency and phase. Figure A3 clearly shows that both the tip vortex and blade surface cavities rotated around the periphery of the inducer inlet with a constant rotating speed which was faster than the inducer rotational speed. The cavity rotating speed tended to decrease with a decrease of the cavitation number, and the cavity length fluctuations almost stopped and steady asymmetric cavitation appeared in an extreme case. In this particular cavitation, three different steady cavity shapes occurred on three blades.

Figure A4 presents the upstream and downstream pressures in the rotating cavitation. The upstream pressure oscillation was very conspicuous and its frequency exactly coincided with that of the cavity rotating speed of the rotating cavitation.

Table A1 Constants of inducers tested

Tip diameter, mm	127.0
Inlet hub diameter, mm	37.0
Outlet hub diameter, mm	65.0
Radial tip clearance, mm	0.5
Number of blades	3
Solidity at tip	2.5
Blade thickness at tip, mm	2.5
Blade thickness at hub, mm	3.5
Inlet blade angle at tip, deg	10.0
Outlet blade angle at tip, deg	12.0
Hub taper angle, deg	21.0

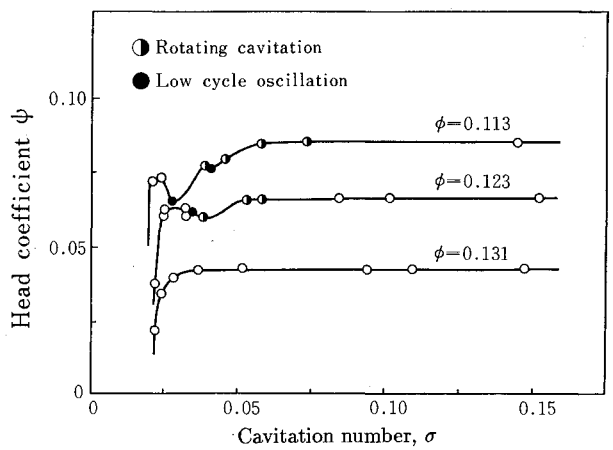

Fig. A1 Suction performance of test inducer.

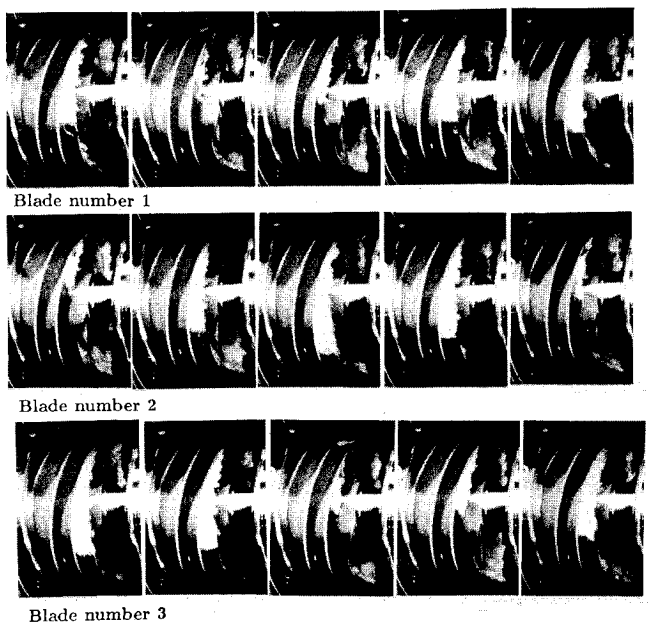

Fig. A2 Sequence of cavity fluctuations on three blades in rotating cavitation. N = 7500 rpm, σ = 0.07, and ϕ = 0.118.

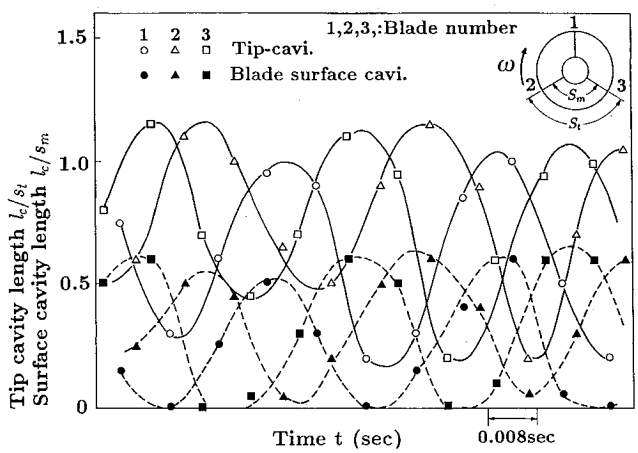

Fig. A3 Fluctuations of cavity length in rotating cavitation.

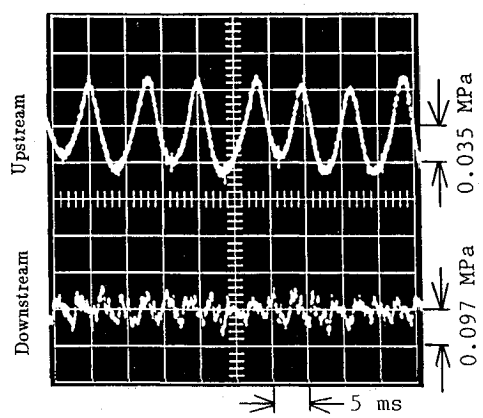

Fig. A4 Pressure oscillations in rotating cavitation.

The downstream pressure oscillation with the same frequency as the upstream pressure oscillation was very small, as shown in Fig. A4, which suggested that rotating cavitation is a phenomena related mainly to flow conditions at the inlet.

Rosenmann[6] measured the inducer hydrodynamic forces under actual operating conditions in order to investigate unexplained shaft deflections observed in many turbopumps operating under partial cavitating conditions. In his experiment,

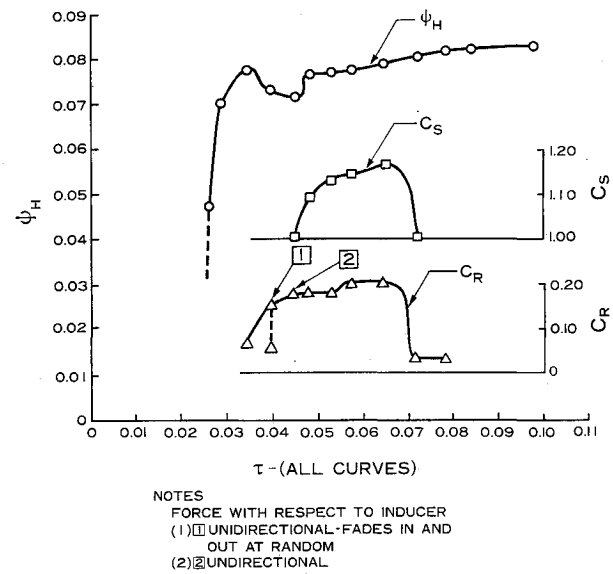

Fig. A5 Shaft forces, head coefficient vs cavitation coefficient.

a flat plate helical inducer with a diameter of 152.4 mm and having three blades was used, the leading-edge tip blade angle β_{t1} was 8.99 deg. Representative data of this experiment are shown in Fig. A5. ψ_H and τ are head coefficient and cavitation parameter [$=(NPSH)2g/U_t^2$], respectively. C_s and C_R are force vector rotation coefficient (ratio of the rotating speed of inducer radial force to shaft rotating speed) and equivalent radial force vector coefficient F_r/F_a, respectively, and F_r and F_a are the approximate inducer axial and radial force, respectively. Figure A5 clearly shows the rotation of inducer radial force in the range of the cavitation parameters of τ = 0.045–0.072. The values of the force vector rotation coefficient ranged from 1.0 to 1.18, which was in good agreement with values of the ratio of cavity rotating speed to the shaft rotational speed in the rotating cavitation mentioned in the previous section. The force vector rotation coefficient gradually decreased along with the decrease of the cavitation parameters. Furthermore, the inducer radial force was present even when the force vector rotation coefficient became equal to one, which exactly corresponds to steady asymmetric cavitation mentioned in the previous section. There were also remarkable degradations of head coefficient near the cavitation parameters where the force vector coefficient was one. This feature is also very similar to that shown in Fig. A1. Judging from the previously mentioned facts, it can be concluded that the rotation of the inducer radial force was caused by rotating cavitation.

Acknowledgment

The authors would like to express their sincere thanks to Y. Sato at Kakuda Research Center of the National Aerospace Laboratory who supported the drawing and preparing of this manuscript.

References

[1]Kurokawa, J., Kamijo, K., and Shimura, T., "Axial Thrust Analysis in LOX-Pump," AIAA Paper 91-2410, June 1991.

[2]Anon., "Liquid Rocket Engine Turbopump Inducer," NASA SP-8052, May 1971.

[3]Davis, R. E., Coons, L. L., and Scheer, D. D., "Internal Stream Flow Analysis for Turbopump Inducers Under Cavitating and Noncavitating Conditions," *Journal of Spacecraft and Rockets*, Vol. 9, No. 2, 1972, pp. 116–122.

[4]Kamijo, K., Shimura, T., and Watanabe, M., "An Experimental Investigation of Cavitating Inducer Instability," American Society of Mechanical Engineers Winter Annual Meeting, 77-WA/FE-14, Atlanta, GA, Nov. 27–Dec. 2, 1977.

[5]Kamijo, K., Shimura, T., and Watanabe, M., "A Visual Obser-

vation of Cavitating Inducer Instability," National Aerospace Lab. (Japan), Rept. NAL TR-598T, May 1980.

[6]Rosenman, W., "Experimental Investigations of Hydrodynamically Induced Shaft Forces with a Three Bladed Inducer," *Proceedings of the Symposium on Cavitation in Fluid Machinery*, American Society of Mechanical Engineers Winter Annual Meeting, Nov. 7–11, 1965, pp. 172–195.

[7]Tsujimoto, Y., Kamijo, K., and Yoshida, Y., "Theoretical Analysis of Rotating Cavitation in Rocket Pump Inducers," AIAA Paper 92-3209, July 1992.

[8]Hans, M. R., and Lloyd, A. W., "ASRDI Oxygen Technology Survey Vol. 1: Thermophysical Properties," NASA SP-3071, 1972.

[9]Stewort, R. B., Jacobsen, R. T., and Myers, A. F., "The Thermodynamical Properties of Oxygen and Nitrogen Part 1—Thermodynamic Properties of Nitrogen from 115R to 3500R with Pressures to 150000 PSIA," NASA CR 128527, 1972.

[10]Acosta, A. J., "An Experimental Study of Cavitating Inducer," *Proceedings of the Second O.N.R. Symposium on Naval Hydrodynamic*, ACR-38, Washington, DC, Aug. 25–29, 1958, pp. 537–557.

[11]Sloteman, D. P., Cooper, P., and Dussord, J. L., "Control of Backflow at the Inlets of Centrifugal Pumps and Inducers," *Proceedings of the 1st International Pump Symposium*, Texas A&M, TX, May 1984, pp. 9–22.

[12]Brennen, C. E., Meissner, C., Lo, E. Y., and Hoffman, G. S., "Scale Effects in the Dynamic Transfer Functions for Cavitating Inducers," *Journal of Fluids Engineering*, Vol. 104, No. 4, 1982, pp. 428–433.

[13]Shimura, T., "The Effects of Geometry in the Dynamic Response of the Cavitating LE-7 LOX Pump," AIAA Paper 93-2126, June 1993.